



**HAL**  
open science

## Optical-fiber-microsphere for remote fluorescence correlation spectroscopy

H. Aouani, F. Deiss, Jérôme Wenger, Patrick Ferrand, N. Sojic, H. Rigneault

► **To cite this version:**

H. Aouani, F. Deiss, Jérôme Wenger, Patrick Ferrand, N. Sojic, et al.. Optical-fiber-microsphere for remote fluorescence correlation spectroscopy. *Optics Express*, 2009, 17 (21), pp.19085-19092. 10.1364/OE.17.019085 . hal-00430201

**HAL Id: hal-00430201**

**<https://hal.science/hal-00430201>**

Submitted on 26 Sep 2015

**HAL** is a multi-disciplinary open access archive for the deposit and dissemination of scientific research documents, whether they are published or not. The documents may come from teaching and research institutions in France or abroad, or from public or private research centers.

L'archive ouverte pluridisciplinaire **HAL**, est destinée au dépôt et à la diffusion de documents scientifiques de niveau recherche, publiés ou non, émanant des établissements d'enseignement et de recherche français ou étrangers, des laboratoires publics ou privés.

# Optical-fiber-microsphere for remote fluorescence correlation spectroscopy

Heykel Aouani<sup>1</sup>, Frédérique Deiss<sup>2</sup>, Jérôme Wenger<sup>1,\*</sup>,  
Patrick Ferrand<sup>1</sup>, Neso Sojic<sup>2</sup> and Hervé Rigneault<sup>1</sup>

<sup>1</sup> Institut Fresnel, CNRS, Aix-Marseille Université, Ecole Centrale Marseille,  
Campus de St Jérôme, 13397 Marseille, France

<sup>2</sup> Institut des Sciences Moléculaires, Université Bordeaux I, ENSCPB, CNRS,  
16 Avenue Pey-Berland, 33607 Pessac, France

\* Corresponding author: jerome.wenger@fresnel.fr

**Abstract:** Fluorescence correlation spectroscopy (FCS) is a versatile method that would greatly benefit to remote optical-fiber fluorescence sensors. However, the current state-of-the-art struggles with high background and low detection sensitivities that prevent the extension of fiber-based FCS down to the single-molecule level. Here we report the use of an optical fiber combined with a latex microsphere to perform FCS analysis. The sensitivity of the technique is demonstrated at the single molecule level thanks to a photonic nanojet effect. This offers new opportunities for reducing the bulky microscope setup and extending FCS to remote or in vivo applications.

© 2009 Optical Society of America

**OCIS codes:** (120.0280) Remote sensing and sensors; (170.6280) Spectroscopy, fluorescence and luminescence; (350.3950) Micro-optics; (120.6200) Spectrometers and spectroscopic instrumentation

---

## References and links

1. S. Maiti, U. Haupts, and W. W. Webb, "Fluorescence correlation spectroscopy: diagnostics for sparse molecules," *Proc. Natl. Acad. Sci. U.S.A.* **94**, 11753-11757 (1997).
2. W. W. Webb, "Fluorescence correlation spectroscopy: inception, biophysical experimentations, and prospectus," *Appl. Opt.* **40**, 3969-3983 (2001).
3. J. Wenger, D. Gérard, H. Aouani, H. Rigneault, B. Lowder, S. Blair, E. Devaux, T. W. Ebbesen, "Nanoaperture-Enhanced Signal-to-Noise Ratio in Fluorescence Correlation Spectroscopy," *Anal. Chem.* **81**, 834-839 (2009).
4. F. Helmchen, "Miniaturization of fluorescence microscopes using fibre optics," *Exp. Physiol.* **87**, 737-745 (2002).
5. J. R. Epstein and D. R. Walt, "Fluorescence-based fibre optic arrays: a universal platform for sensing," *Chem. Soc. Rev.* **32**, 203-214 (2003).
6. O. S. Wolfbeis, "Fiber-optic chemical sensors and biosensors," *Anal. Chem.* **78**, 3859-3873 (2006).
7. K. Garai, M. Muralidhar, and S. Maiti, "Fiber-optic fluorescence correlation spectrometer," *Appl. Opt.* **45**, 7538-7542 (2006).
8. K. Garai, R. Sureka, and S. Maiti, "Detecting amyloid-beta aggregation with fiber-based fluorescence correlation spectroscopy," *Biophys. J.* **92**, L55-L57 (2007).
9. Y.-C. Chang, J. Y. Ye, T. Thomas, Y. Chen, J. R. Baker, and T. B. Norris, "Two-photon fluorescence correlation spectroscopy through dual-clad optical fiber," *Opt. Express* **16**, 12640-12649 (2008).
10. Z. Chen, A. Taflove, and V. Backman, "Photonic nanojet enhancement of backscattering of light by nanoparticles: a potential novel visible-light ultramicroscopy technique," *Opt. Express* **12**, 1214-1220 (2004).
11. X. Li, Z. Chen, A. Taflove, and V. Backman, "Optical analysis of nanoparticles via enhanced backscattering facilitated by 3-D photonic nanojets," *Opt. Express* **13**, 526-533 (2005).
12. P. Ferrand, J. Wenger, M. Pianta, H. Rigneault, A. Devilez, B. Stout, N. Bonod, and E. Popov, "Direct imaging of photonic nanojets," *Opt. Express* **16**, 6930-6940 (2008).
13. A. Heifetz, K. Huang, A. V. Sahakian, X. Li, A. Taflove, V. Backman, "Experimental confirmation of backscattering enhancement induced by a photonic jet," *Appl. Phys. Lett.* **89**, 221118 (2006).

14. D. Gérard, J. Wenger, A. Devilez, D. Gachet, B. Stout, N. Bonod, E. Popov, H. Rigneault, "Strong electromagnetic confinement near dielectric microspheres to enhance single-molecule fluorescence," *Opt. Express* **16**, 15297-15303 (2008).
  15. D. Gérard, A. Devilez, H. Aouani, B. Stout, N. Bonod, J. Wenger, E. Popov, and H. Rigneault, "Efficient excitation and collection of single molecule fluorescence close to a dielectric microsphere," *J. Opt. Soc. Am. B* **26**, 1473-1478 (2009).
  16. A. Devilez, N. Bonod, B. Stout, D. Gérard, J. Wenger, H. Rigneault, and E. Popov, "Three-dimensional subwavelength confinement of photonic nanojets," *Opt. Express* **17**, 2089-2094 (2009).
  17. J. Wenger, D. Gérard, H. Aouani, and H. Rigneault, "Disposable microscope objective lenses for fluorescence correlation spectroscopy using latex microspheres," *Anal. Chem.* **80**, 6800-6804 (2008).
  18. A. Gennerich and D. Schild, "Fluorescence Correlation Spectroscopy in Small Cytosolic Compartments Depends Critically on the Diffusion Model Used," *Biophys. J.* **79**, 3294-3306 (2000).
  19. J. Wenger, D. Gérard, N. Bonod, E. Popov, H. Rigneault, J. Dintinger, O. Mahboub and T. W. Ebbesen, "Emission and excitation contributions to enhanced single molecule fluorescence by gold nanometric apertures," *Opt. Express* **16**, 3008-3020 (2008).
  20. M. Pitschke, R. Prior, M. Haupt, and D. Riesner, "Detection of single amyloid  $\beta$ -protein aggregates in the cerebrospinal fluid of Alzheimer's patients by fluorescence correlation spectroscopy," *Nature Medicine* **4**, 832-834 (1998).
  21. N. Opitz, P. J. Rothwell, B. Oeke, and P. Schwill, "Single molecule FCS-based oxygen sensor ( $O_2$ -FCSensor): a new intrinsically calibrated oxygen sensor utilizing fluorescence correlation spectroscopy (FCS) with single fluorescent molecule detection sensitivity," *Sensors and Actuators B* **96**, 460-467 (2003).
  22. F. H. C. Wong, D. S. Banks, A. Abu-Arish, and C. Fradin, "A Molecular Thermometer Based on Fluorescent Protein Blinking," *J. Am. Chem. Soc.* **129**, 10302-10303 (2007).
- 

## 1. Introduction

Fluorescence correlation spectroscopy (FCS) is a powerful and versatile method for the detection and characterization of fluorescent molecules [1, 2]. FCS is based on computing the temporal correlation of the fluorescence intensity fluctuations. It can in principle provide information about any molecular process that induces a change in the fluorescence intensity. Applications include determining translational and rotational diffusion, molecular concentrations, chemical kinetics, and binding reactions.

In contrast to other fluorescence techniques, the critical parameter in FCS is not the total fluorescence intensity, but the amplitude of the fluorescence fluctuations, which is directly related to the brightness of each molecule. While computing the temporal correlation of the fluorescence intensity, non-zero correlations will occur only if they originate from the same molecule. This highlights the single molecule nature of FCS, and the need to maximize the detected photons from each molecule [3].

Therefore, FCS is commonly implemented on a confocal microscope with a high numerical aperture objective. Despite its extreme sensitivity (down to the single molecule in a routine experiment), this approach remains expensive and difficult to integrate onto a lab-on-a-chip format because of the bulky optical arrangement.

Much attention is currently devoted to miniaturize optical devices and extend the detection capabilities to remote or in vivo applications. To this end, the use of an optical fiber probe for simultaneous excitation and detection of fluorescent molecules is a promising approach [4, 5, 6], which would be greatly extended if FCS was implemented for dynamics analysis.

Recently, the use of a single-mode [7, 8] or dual-clad [9] optical fiber has been investigated to perform FCS with one- or two-photon excitation respectively. However, due to low detected fluorescence rates per molecule and the high background in the fibers, these demonstrations were limited to detecting fluorescent nanospheres of at least 24 nm in diameter. Extending the technique to true single-molecule sensitivity remains a challenge.

Here, we circumvent the aforementioned limitations by combining the optical fiber endoscope with a polystyrene microsphere at the end of the fiber (figure 1). Selective wet-chemical etching of the distal face of an optical fiber bundle produces a microwell array. The microwells

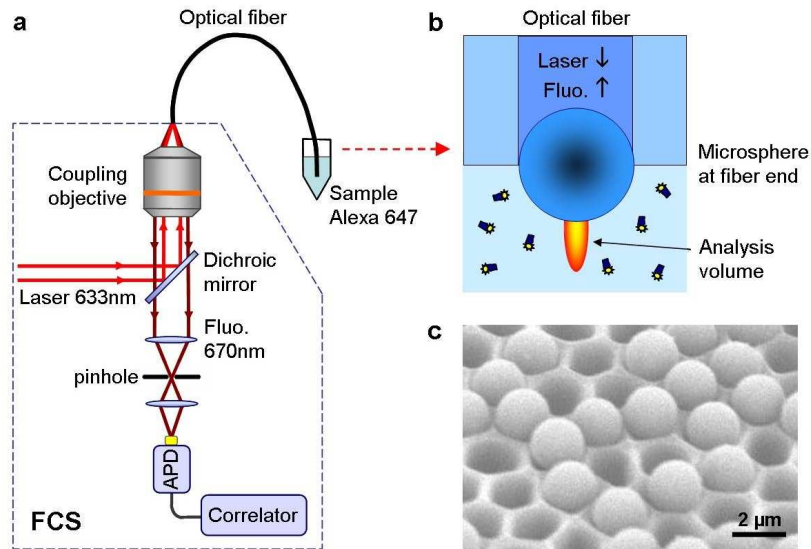


Fig. 1. (a) Schematic view of the experimental setup. (b) shows a close-up view of the end of the optical fiber core covered with the microsphere. (c) Electron microscope image of the optical fiber bundle output partly etched with polystyrene microspheres.

correspond to the etched optical cores, and are then filled with microspheres. This procedure enables correct alignment of the microsphere on top of the optical fiber.

We call this device OFM, which stands for Optical-Fiber-Microsphere. By acting as a microlens coupler directly set at the fiber end, the microsphere enables efficient excitation and detection of the fluorescence from standard single molecular dyes. This enables the first demonstration of remote fiber-based FCS at the single molecule level.

Our results are strongly related to the peculiar electromagnetic field distribution that emerges from a dielectric microsphere. Under plane wave illumination, several recent papers have theoretically and experimentally demonstrated the existence of a beam called “photonic nanojet” that emerges from the microsphere with high intensity, subwavelength transverse dimensions and low divergence [10, 11, 12]. Dielectric microspheres have appeared as effective devices to enhance nanoparticle backscattering [13], and single molecule fluorescence detection in a conventional confocal microscope setup [14, 15, 16].

We have recently demonstrated that a latex microsphere combined with a simple lens can form a high performance disposable optical system, offering a simple and low-cost alternative to the expensive microscope objectives used in FCS [17]. However, this method requires careful positioning of the microsphere respectively to the collection lens focus, and is not compatible with an integrated arrangement for remote sensing.

Here, we take advantage of the previous demonstrations to describe an optical fiber-microsphere (OFM) coupled system with single molecule sensitivity for FCS. This device has the advantage to operate without any positioning stage (except the fiber input coupler), and to offer remote sensing capabilities in a compact setup.

## 2. Numerical simulations of the optical fiber microsphere system

To investigate the interaction between the optical fiber mode and the microsphere, we have performed 2D finite-difference time-domain (FDTD) computations using RSoft Fullwave soft-

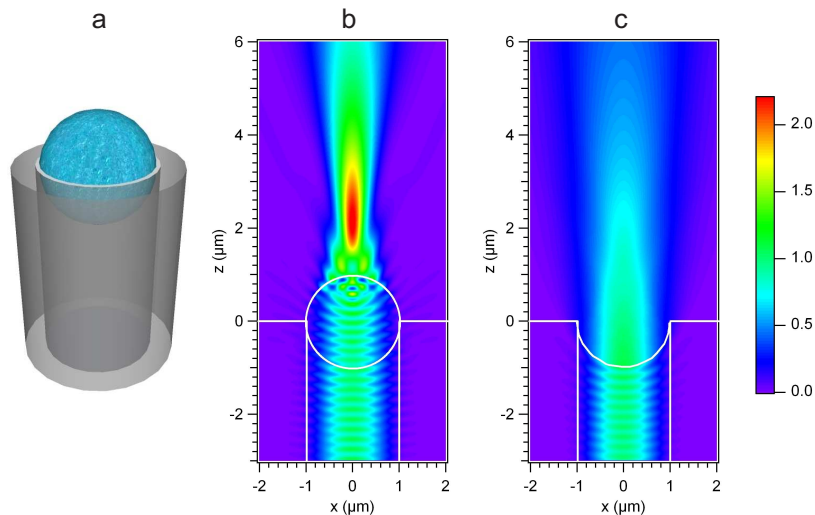


Fig. 2. (a) Experimental configuration of the fiber core-clad and microsphere configuration. FDTD-calculated electric field intensity with (b) and without (c) a  $2\ \mu\text{m}$  cylinder illuminated by the fundamental fiber mode at  $\lambda = 633\ \text{nm}$  (see text for structure details).

ware (Fig. 2). These simulations are intended to give a vision of the peculiar electromagnetic distribution that emerges from this system.

The computational domain is set to  $4 \times 8\ \mu\text{m}^2$ , with  $10 \times 10\ \text{nm}^2$  grid size and perfectly matched layers as boundary conditions. The microsphere is modelled by a dielectric cylinder with a  $2\ \mu\text{m}$  diameter and a refractive index corresponding to polystyrene in the visible range  $n = 1.59$ . The  $\text{GeSiO}_2$ - $\text{FSiO}_2$  core-clad optical fiber has a core diameter of  $2\ \mu\text{m}$  (refractive index 1.49) and cladding diameter of  $3.4\ \mu\text{m}$  (refractive index 1.43). The embedding medium is taken to be water (refractive index 1.33).

The fundamental mode of the optical fiber at 633 nm wavelength (in vacuum) is launched inside the fiber. When the microsphere is set on top of the fiber (Fig. 2(b)), the incident beam is focused in close fashion to photonic nanojets under plane wave illumination [10, 11]. When no sphere is present (Fig. 2(c)), the beam is just diverging from the chemically etched fiber output.

From Fig. 2(b), we estimate the transverse and axial FWHM of 480 nm and  $2.7\ \mu\text{m}$  respectively, which come close to the values typically reached with a high NA microscope objective. The specific focusing brought by the microsphere further confines the excitation light. Reciprocally, the microsphere also allows for collecting the fluorescence light [15]. Both effects contribute to the increased sensitivity of the OFM system.

### 3. Materials and methods

#### 3.1. Optical fibers and microspheres

The bundles consist of 6000 individually cladded optical fibers coherently organized in an imaging area of  $270\ \mu\text{m}$  diameter (FIGH-06-300S, Fujikura Ltd). The two faces of the 50 cm imaging fiber are polished before use with 5-1-0.3  $\mu\text{m}$  lapping films (Thorlabs). A microwell at each optical fiber core is realized by a 25 s chemical etching in a fluorhydric acid solution (use with caution: HF solutions are extremely corrosive), using the difference in wet-etching rates between the  $\text{GeO}_2$ -doped core and the fluorine-doped cladding. The reaction time was adapted to create wells fitting the  $2\ \mu\text{m}$  polystyrene spheres. The OFM is finally obtained by solvent

evaporation of a solution containing the microspheres: Small drops of this solution are successively deposited on the etched face and let dry to allow the microspheres to self-organize on the microwell array. Last, distilled water is used to wash out the unfixed microspheres.

### 3.2. FCS experimental setup

As molecular probe, we use Alexa Fluor 647 (A647, Invitrogen, Carlsbad, CA) which is a commonly used dye for FCS with absorption / emission maxima at 650 and 670 nm. Our experimental setup is based on an inverted microscope with a Zeiss C-Apochromat 40x/NA 1.2/ water-immersion objective, providing a state-of-the-art reference for confocal FCS setup. For experiments with the bundle of fibers, the same objective is used to couple the 633 nm excitation light into the fiber and collect the emitted fluorescence. However, to get a better coupling into a single fiber of the bundle, the size of the incident beam is reduced to obtain an effective NA of 0.3. Micrometer positioning of the fiber bundle with respect to the microscope objective focus enables exciting a single fiber. We emphasize that no cross-correlation between different fibers of the bundle was detected, thanks to a 4  $\mu\text{m}$  separation between each individual fiber and 50 cm propagation length.

The fluorescence path after the fiber comprises a dichroic mirror (Omega Filters 650DRLP) followed by a confocal filter with a 50  $\mu\text{m}$  pinhole. Detection is performed by two fast avalanche photodiodes (Micro Photon Devices by PicoQuant MPD-5CTC) separated by a 50/50 beamsplitter. Due to a strong Raman and fluorescence background from the optical fiber, A647 fluorescence measurements are spectrally integrated in a narrow window around  $680 \pm 10$  nm by combining two bandpass filters (Omega Filters 670DF40 and 695AF55). This configuration is set to optimize the fluorescence signal-to-noise ratio.

Finally to perform FCS, the fluorescence intensity temporal fluctuations are analyzed by cross-correlating the signal of the two photodiodes with a ALV6000 hardware correlator. This computes the correlation function:  $g^{(2)}(\tau) = \langle F(t) \cdot F(t + \tau) \rangle / \langle F(t) \rangle^2$ , where  $\langle \cdot \rangle$  stands for time-averaging over the experiment duration [2]. This well-known configuration eliminates correlations due to the dead time of the photodiodes and avoids artifacts. Each individual FCS measurement was obtained by averaging at least 10 runs of 10 s duration each.

### 3.3. FCS analysis

To analyze the FCS data we use the analytical model established for Brownian three-dimensional diffusion in the case of a Gaussian molecular detection efficiency [2]:

$$g^{(2)}(\tau) = 1 + \frac{1}{N} \left(1 - \frac{B}{F}\right)^2 \left[1 + n_T \exp\left(-\frac{\tau}{\tau_T}\right)\right] \frac{1}{(1 + \tau/\tau_d) \sqrt{1 + s^2 \tau/\tau_d}} \quad (1)$$

where  $N$  is the average number of molecules,  $F$  the total signal,  $B$  the background noise,  $n_T$  the amplitude of the dark state population,  $\tau_T$  the dark state blinking time,  $\tau_d$  the mean diffusion time and  $s$  the ratio of transversal to axial dimensions of the analysis volume, fixed here to  $s = 0.2$  from the numerical simulations. Strictly speaking, the assumptions for the above model are not fulfilled close to a microsphere. However, let us point out that restriction of the range available for diffusion will only slightly affect the diffusion time (millisecond time range), and leave unaffected the correlation amplitude and the fast components of the correlogram [18]. Equation (1) model has successfully been applied in more complex systems [14, 19]. Lastly, we point out that relative measurements of variations in diffusion times are always possible, and are sufficient to assess enzymatic activity, chemical rate constants, or binding rates.

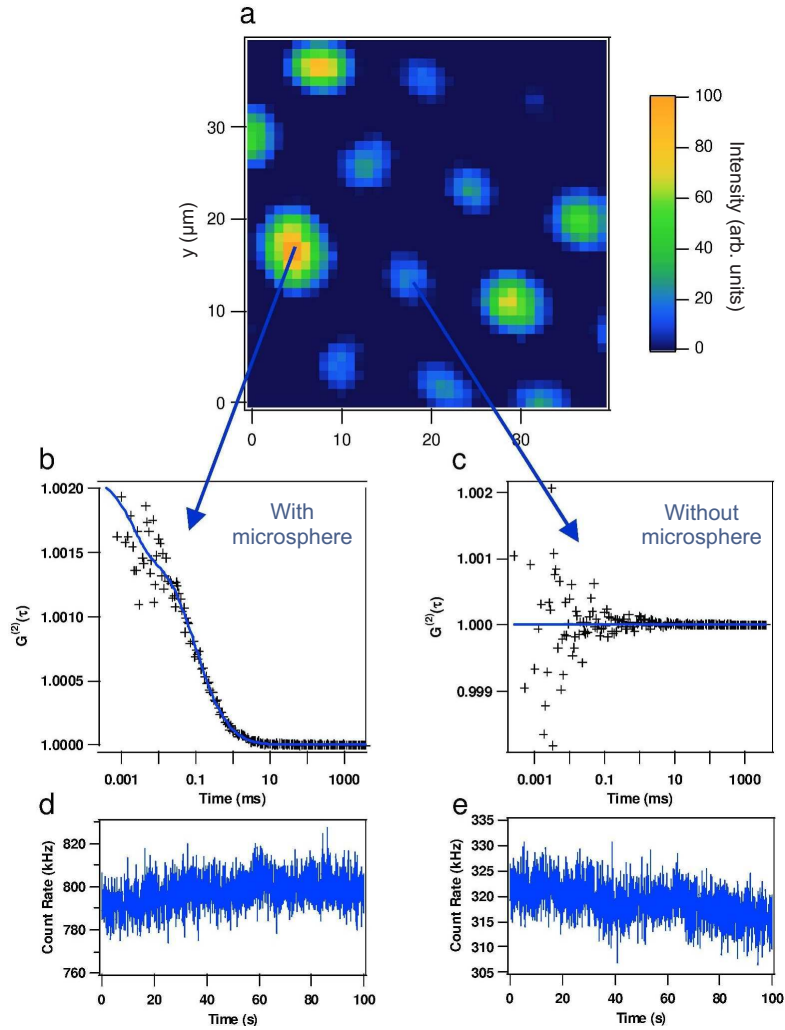


Fig. 3. (a) Scanning image of the bundle: bright areas correspond to the presence of microsphere, where autocorrelation function is obtained (b). Analysis of the correlation function in (b) yield:  $N = 284$ ,  $\tau_d = 123\mu s$ ,  $s = 0.2$ ,  $n_T = 0.39$ ,  $\tau_T = 2\mu s$ ,  $CRM = 1.9\text{kHz}$ , the laser power being set to 0.6 mW at the entrance of the fiber. Without microsphere (dark areas), FCS measurements cannot be performed (c). (d) and (e) are the fluorescence signal traces corresponding respectively to (b) and (c).

#### 4. Experimental results and discussion

We conduct FCS measurements by dipping the OFM bundle into a fluorescent solution of A647 molecules. Not all etched fibers are associated with a  $2\mu\text{m}$  polystyrene sphere, as the microsphere deposit step was not specifically optimized for this study. Scanning the coupling into the bundle is thus necessary to identify optical fiber-microsphere coupled systems (Fig. 3 (a)). The bright areas correspond to the presence of a  $2\mu\text{m}$  sphere on the fiber output where the fluorescence correlation function is clearly greater than one (Fig. 3 (b)) while in dark areas, no time correlation was found, corresponding to the absence of microsphere (Fig. 3 (c)).

From Figure 3 (b) it is apparent that thanks to the microsphere, the sensitivity is high enough to detect temporal correlations for FCS with standard organic fluorophores. As demonstrated in the negative control in Fig. 3 (c) and (e) and discussed further below, the correlations observed in the case of the microsphere are related to the detection of A647 molecules, and not to any fluctuation originating from technical noise on our setup.

To analyse the FCS data according to Eq. (1), it is crucial to accurately determine the background noise  $B$ . In our case,  $B$  originates mainly from fluorescence and Raman scattering from impurities or dopants in the fibers. Special care has been taken to evaluate the level of this background noise by dipping the fibers into pure water solution. The typical level of background noise corresponding to the situation of Fig. 3 is  $B = 270$  kHz, the signal-to-noise ratio is typically about 1.9.

Table 1 summarizes the characteristics of the OFM system, and compares the results to the conventional confocal setup using a 1.2 NA microscope objective, with the same A647 solution. Very nicely, the measured numbers of molecules come very close for both systems. This demonstrates that the analysis volume with the OFM is comparable to the one obtained with a diffraction-limited state-of-the-art FCS microscope, and stands in good agreement with the numerical simulations performed in Section 2. Despite a much higher background in the case of the OFM, the sensitivity is still high enough to detect single A647 molecules within a reasonable integration time.

Table 1. Results of the numerical fits of the FCS data measured with the Zeiss objective and OFM. The observation volume  $V_{eff}$  is inferred from the number of molecules  $N$  and the dye concentration.

Objective	$N$	$\tau_d$ ( $\mu$ s)	$V_{eff}$ (fL)	CRM (kHz)	$P_{laser}$ (mW)
Zeiss 1.2NA	222	115	0.5	3.5	0.1
OFM	284	123	0.65	1.9	0.6

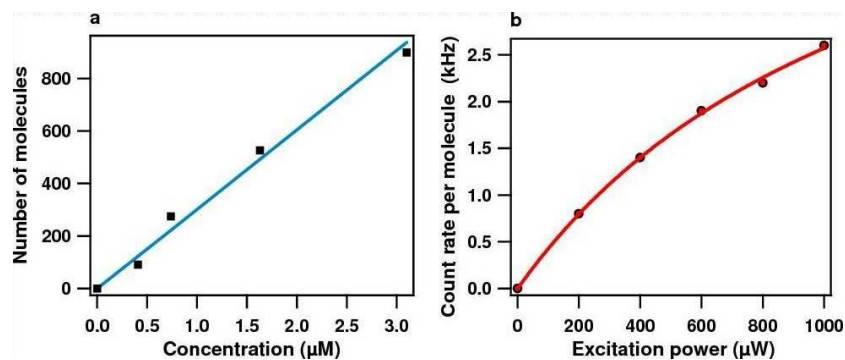


Fig. 4. (a) Evolution of the detected number of A647 molecules versus calibrated molecular concentration. (b) Count rate per molecule plotted versus excitation power (circle) and numerical fit (solid line).

To discuss the concentration sensitivity of the OFM, we carried out FCS measurements for different calibrated concentrations of A647 ranging from 0.4 to 3.1  $\mu$ M. Figure 4 (a) displays the evolution of the total number of molecules detected with the OFM versus the concentra-



tion of A647 dye. As expected for FCS, the detected number of molecules follows a linear relationship with the concentration. Due to the high background noise, FCS measurements are presently limited to concentrations above 400 nM.

In addition, we performed a set of FCS measurements of the detected count rates per molecule  $CRM$  while increasing the excitation power from 200 to 1000  $\mu\text{W}$  (Fig. 4 (b)). This experimental data follows the standard expression of the fluorescence rate of a three level system given by  $CRM = AI_e/(1 + I_e/I_s)$ , where  $I_e$  is the excitation intensity,  $I_s$  the saturation intensity, and  $A$  a constant proportional to the dye's absorption cross section, its quantum yield, and the setup collection efficiency [19]. Results of the fit are:  $A = 0.05 \text{ kHz}/\mu\text{W}$ ,  $I_s = 1260 \mu\text{W}$ . This measurement provides another confirmation of the single-molecule sensitivity of the OFM.

## 5. Conclusions

We report the use of an Optical-Fiber-Microsphere (OFM) which combines an etched optical fiber with a latex microsphere to perform remote fiber-based FCS analysis at the single molecule level. Thanks to the microsphere, the excitation beam is further focused and the fluorescence collection efficiency is improved. This configuration circumvents the drawbacks introduced while performing remote FCS sensing with an optical fiber, and enables a sensitivity high enough to work with standard fluorescent molecules.

We point out that there is no need to use a bundle; a single optical fiber combined with a 2  $\mu\text{m}$  sphere can achieve the same performances. FCS measurements have been performed by using an optical fiber combined with 3  $\mu\text{m}$  latex sphere, but no correlation of the fluorescence signal was found due to a weaker focusing by these spheres. Currently, the main limitation of the OFM is the intrinsic background fluorescence of the fiber that makes FCS studies on A647 difficult below 400 nM concentration. Using fibers with less background noise and/or brighter dyes could further extend FCS studies at nanomolar concentration.

We believe that OFM offers new opportunities for remote or in vivo fluorescence characterization together with a miniaturization of bulky FCS setup. Compact portable systems for FCS analysis appear clearly feasible with this technique. We foresee new investigations for endoscopic applications, and opto-microfluidic lab-on-chips. Applications for remote sensing with FCS concern for instance early diagnosis of Alzheimer's disease [20], oxygen sensing [21], or temperature sensing [22].

## Acknowledgments

The authors acknowledge stimulating discussions with D. Gérard, N. Bonod, A. Devilez, B. Stout, and E. Popov. This work is funded by contract ANR-07-NANO-006-03 "ANTARES".